



ROOM 102D
10:18-10:36

SESSION 10D03 – Modeling & Computation in Energy & the Environment

CFD MODELING OF A MOLTEN SLAG JET FREE SURFACE FLOW DURING MINERAL WOOL FIBERIZATION



Minneapolis, MN, Tuesday the 18th of October, 2011

**11 AIChE**
Annual Meeting, Minneapolis, MN

Dr. DIMITRIOS I. GEROGIORGIS
Prof. DIMITRIOS PANIAS
Prof. IOANNIS PASPALIARIS



OUTLINE OF PRESENTATION

- Mineral wool fiberization - Mathematical modeling strategy
- Thermophysical properties of molten slag: Literature review
- Dimensional Analysis: Deriving dimensionless numbers
- CFD analysis of nonisothermal free surface vertical flow
- Conclusions on process design and future research goals

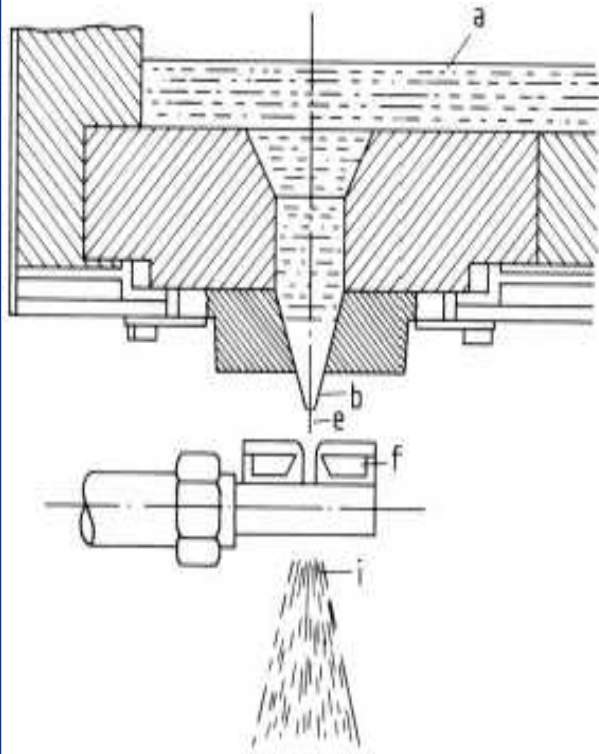


AGENDA

- Mineral wool fiberization - Mathematical modeling strategy
- Thermophysical properties of molten slag: Literature review
- Dimensional Analysis: Governing dimensionless numbers
- CFD analysis of nonisothermal vertical free surface flow
- Conclusions on process design and future research goals

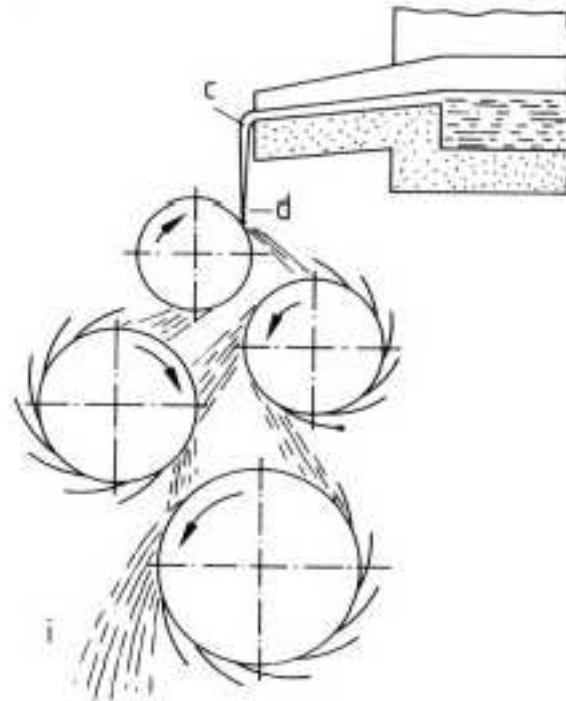


CONVENTIONAL MINERAL FIBERIZATION PROCESSES



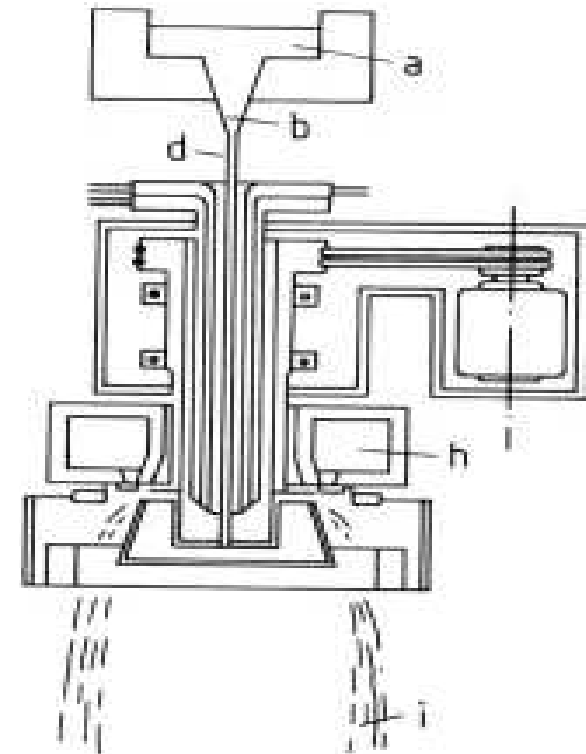
OWENS PROCESS

- Air/steam melt-blowing process
- Melt emerging from Pt crucible
- Use of downward gas jet
- Fiber length: 3 – 10 cm



ROCK WOOL PROCESS

- One-step centrifugal process
- Melt distribution @ 1st cylinder
- Multiple rotating cylinders
- Fiber length: 3 – 10 cm

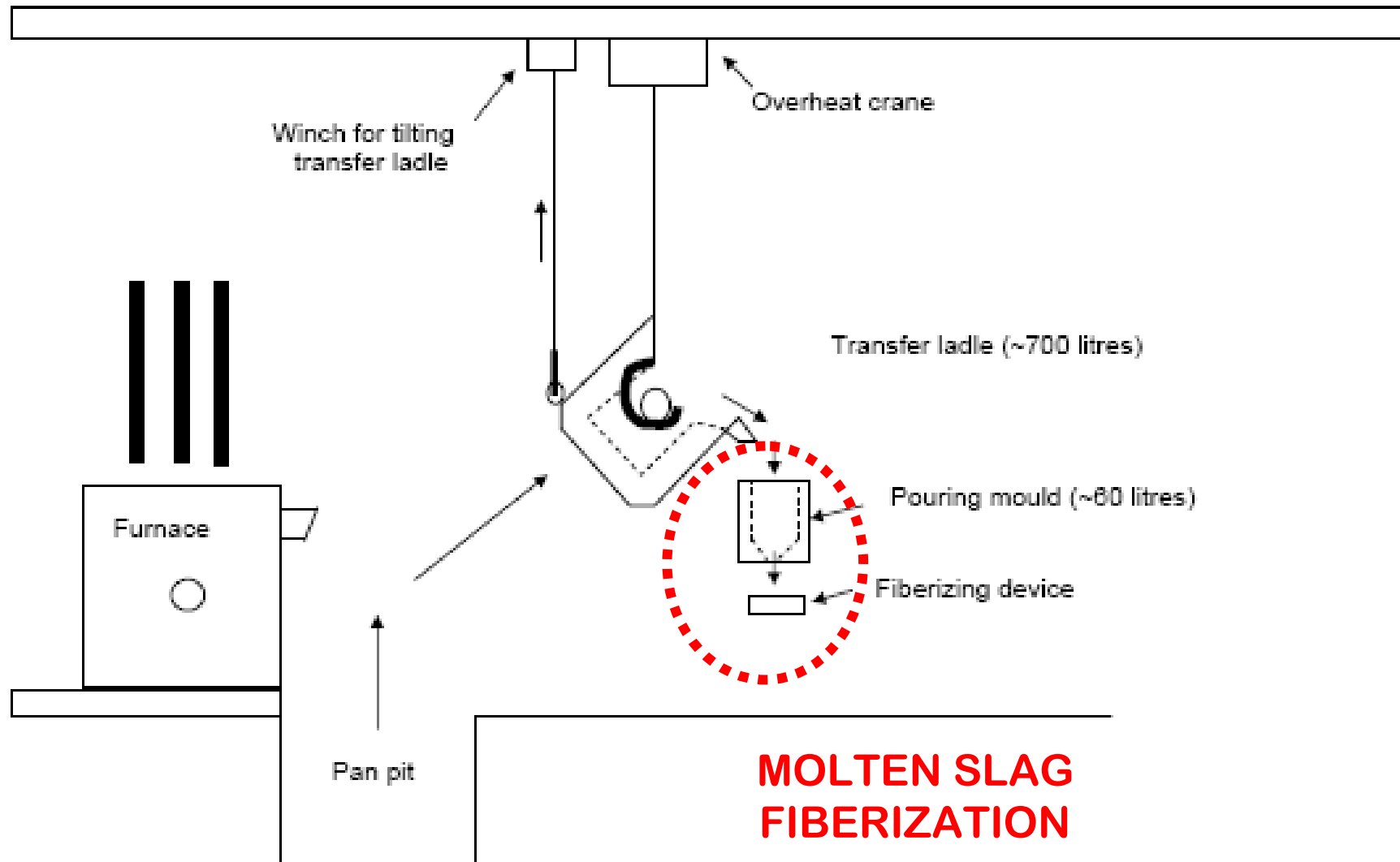


ROTARY PROCESS

- Two-step rotary process
- Rotating Pt/steel melt distributor
- Entrainment by combustion gases
- Fiber diameter: 3 – 6 μm



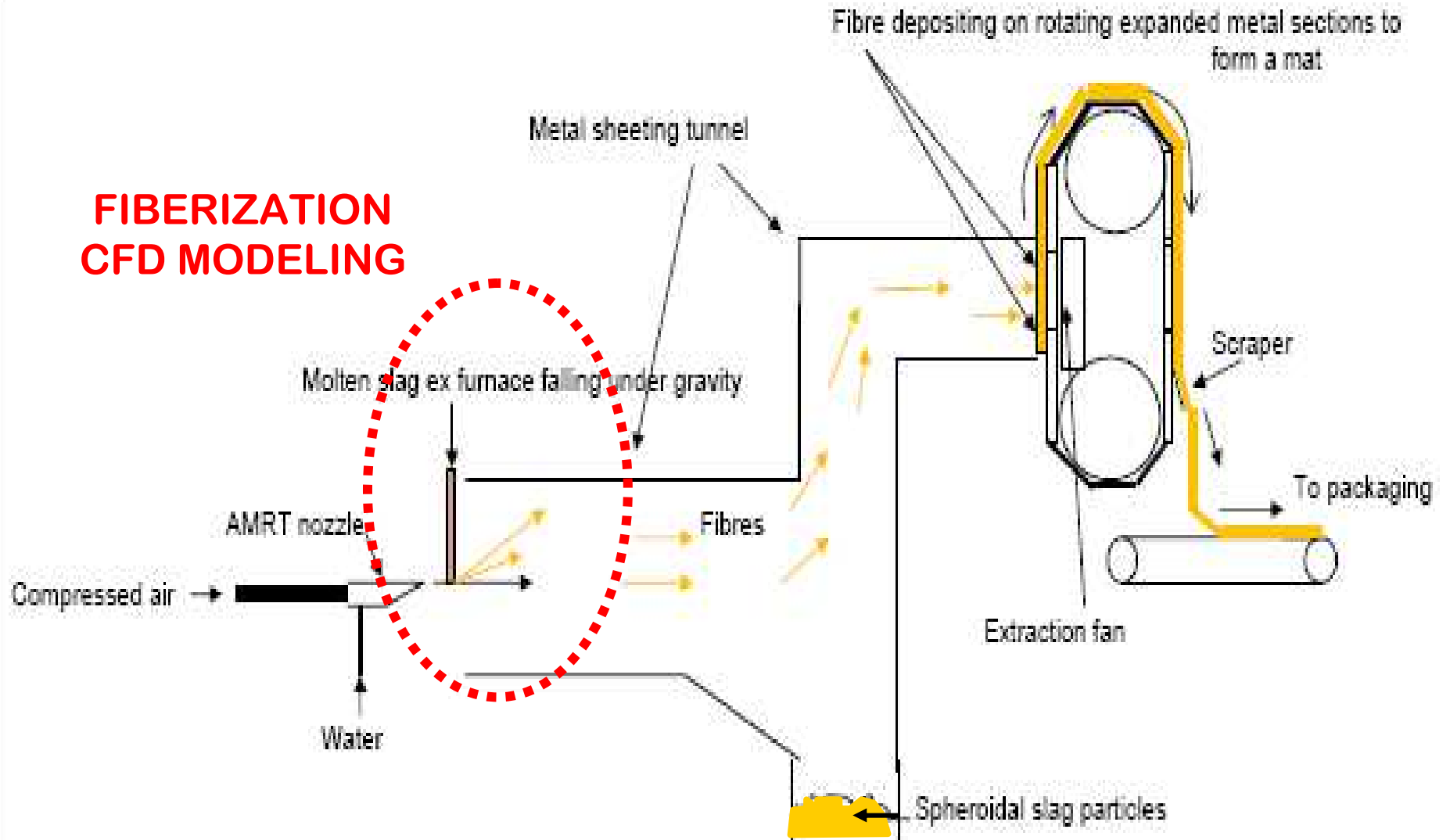
MOLTEN SLAG HANDLING PROCESS: SCHEMATIC





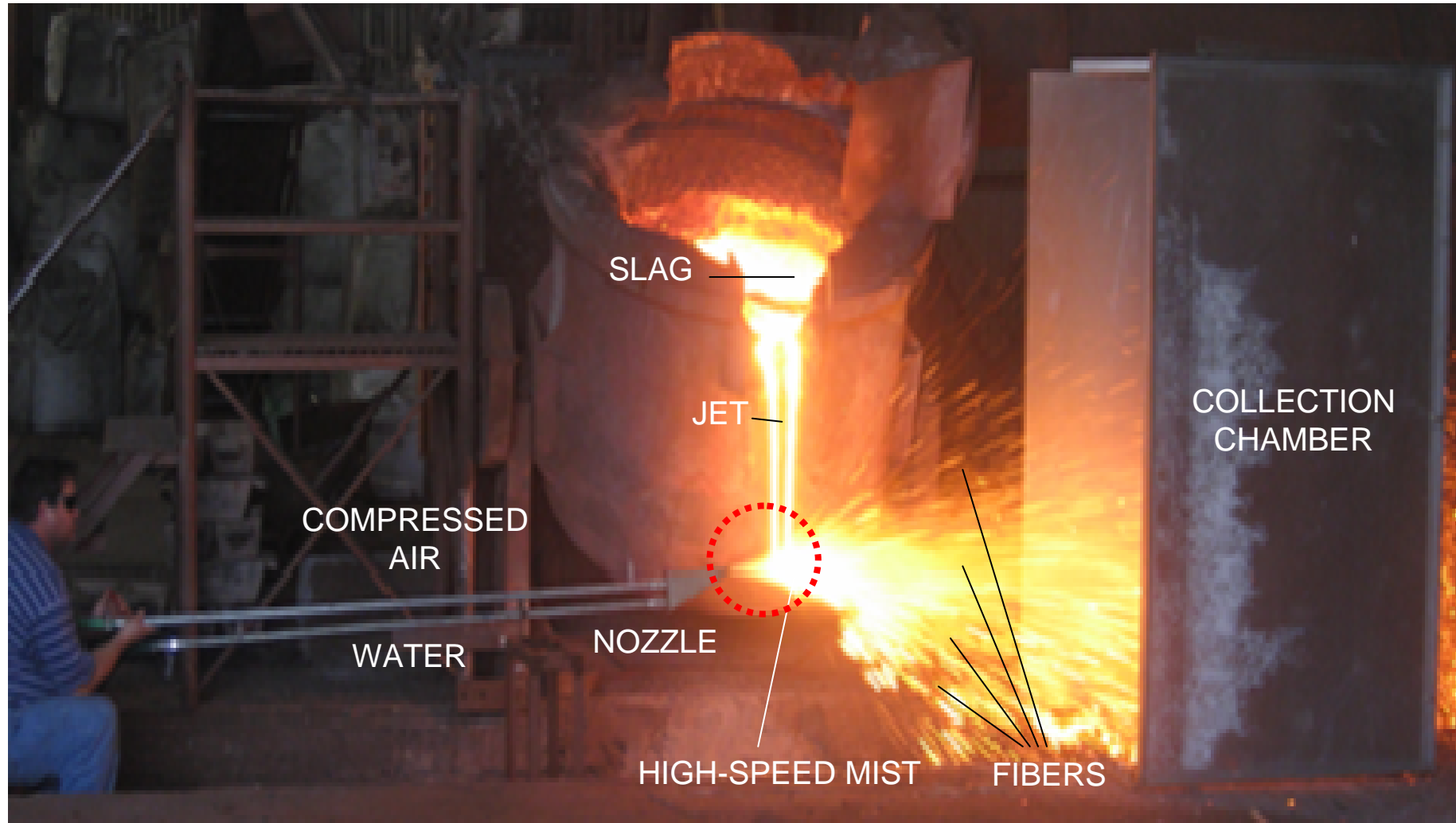
MINERAL WOOL FIBERIZATION: SCHEMATIC

FIBERIZATION CFD MODELING





MINERAL WOOL FIBERIZATION: PROCESS OVERVIEW



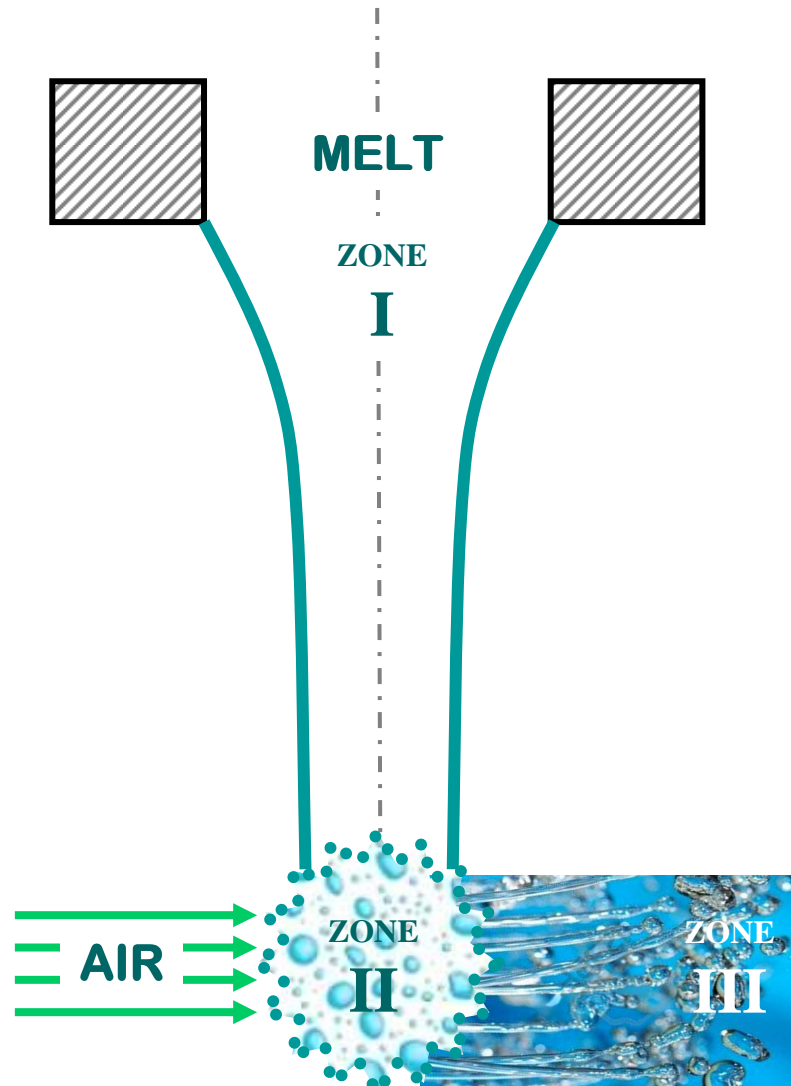


MINERAL SLAG FIBERIZATION: VIDEO OF THE PROCESS





MINERAL WOOL FIBERIZATION MODELING: STRATEGY



ZONE I: MOLTEN SLAG BULK FLOW

Macroscopic free surface laminar flow zone
Nonisothermal field (molten slag jet cooling)
St. state homogeneous field, high observability

ZONE II: MINERAL FIBER GENERATION

Microscopic molten slag fiber generation zone
Isothermal field (very low residence time)
Dynamic inhomogeneous field, low observability

ZONE III: DISPERSED FLOW OF FIBERS

Macroscopic dispersed flow zone
Nonisothermal field (fiber cooling+elongation)
Dynamic inhomogeneous field, med observability



AGENDA

- Mineral wool fiberization - Mathematical modeling strategy
- Thermophysical properties of molten slag: Literature review
- Dimensional Analysis: Governing dimensionless numbers
- CFD analysis of nonisothermal vertical free surface flow
- Conclusions on process design and future research goals



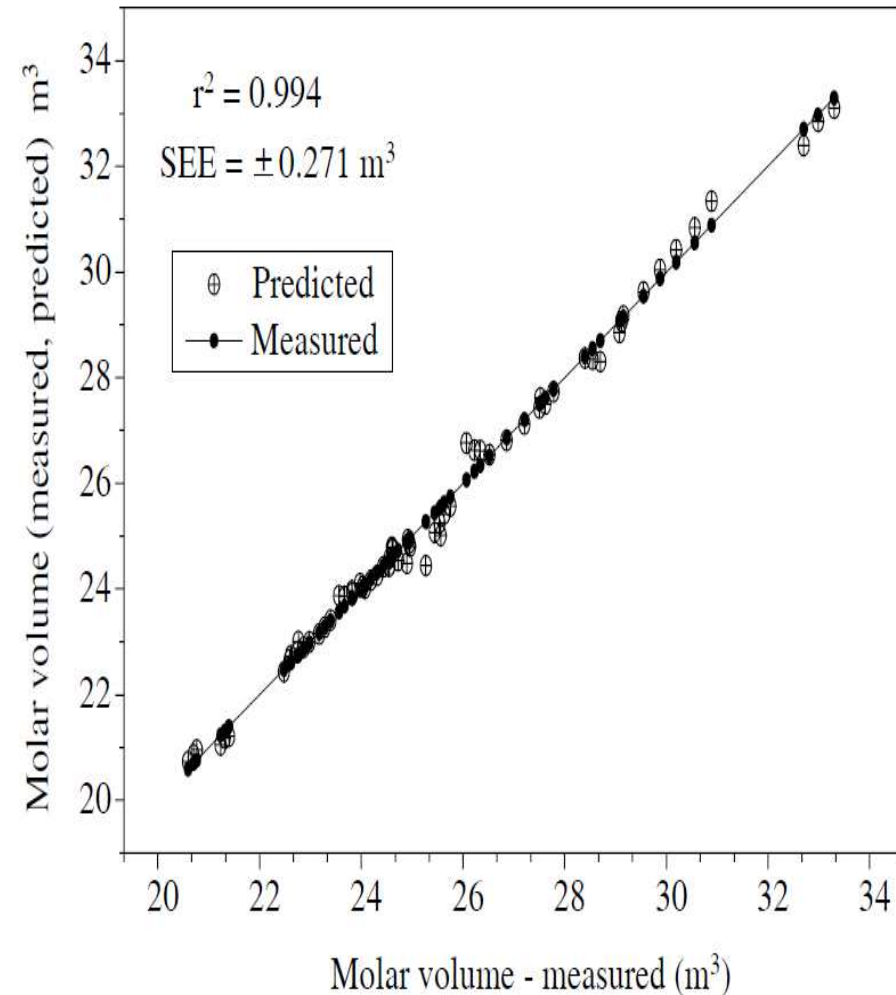
DENSITY OF SILICATE MELTS (Sirok et al., 2005)

$$\rho_L = \frac{M_L}{V_L} = \frac{\sum_{i=1}^N x_i M_i}{\sum_{i=1}^N x_i V_i}$$

$$V_L(T) = \sum_{i=1}^{N=9} x_i \cdot V_{i,1773} + \sum_{i=1}^{N=9} x_i \cdot (\partial V_i / \partial T)(T - 1773) = \dots$$

$$= \sum_{i=1}^{N=9} x_i \cdot \varepsilon_i + \sum_{i=1}^{N=9} x_i \cdot \mu_i \cdot (T - 1773)$$

Oxide	SiO ₂	TiO ₂	Al ₂ O ₃	Fe ₂ O ₃	FeO
v _i	25.178	24.227	39.126	44.457	11.731
μ _i	-0.0025	0.0027	-0.0096	-0.0229	0.0138
Oxide	MgO	CaO	Na ₂ O	K ₂ O	
v _i	14.110	18.677	35.872	49.978	
μ _i	0.0041	0.0081	0.0158	0.0190	





DENSITY OF SILICATE MELTS: SLAG RESULTS (10^3 kg.m^{-3})

T (°C)	STOICH.	5.0 % C	7.5 % C	10.0 % C	TARGET
1300	<u>2.755</u>	2.713	2.709	2.712	2.664
1400	2.740	2.703	2.701	2.705	2.648
1500	2.726	2.693	2.692	2.699	2.633
1600	2.711	2.683	2.684	2.692	2.618
1700	2.697	2.674	2.676	2.685	2.604
1800	2.683	2.664	2.668	2.678	<u>2.589</u>



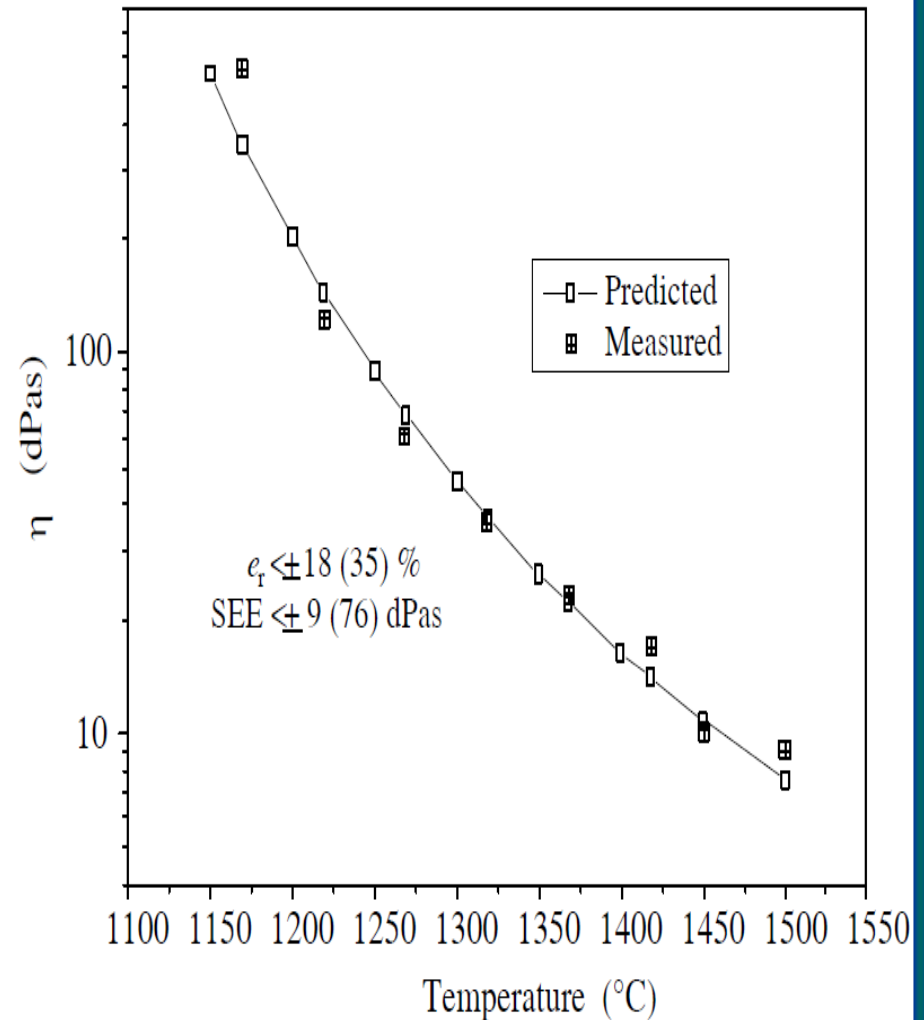
VISCOSITY OF SILICATE MELTS (Sirok et al., 2005)

LAKATOS method

$$\log \eta = B_0 + \frac{B_1}{T + T_0}$$

$$T = A \left(\frac{b_0 - SiO_2 - b_1 \cdot Al_2O_3}{b_2 \cdot CaO + b_3 \cdot MgO + b_4 \cdot Alk + b_5 \cdot FeO + b_6 \cdot Fe_2O_3} \right)$$

Coefficient	$\log \eta = 1.5$	$\log \eta = 2.0$	$\log \eta = 2.5$
A	1375.76	1272.64	1192.44
b_0	122.29	117.64	112.99
b_1	1.06247	1.05336	1.03567
b_2	1.57233	1.42246	1.27336
b_3	1.61648	1.48036	1.43136
b_4	1.44738	1.51099	1.41448
b_5	1.92899	1.86207	1.65966
b_6	1.47337	1.36590	1.20929





VISCOSITY OF SILICATE MELTS (Browning et al., 2003)

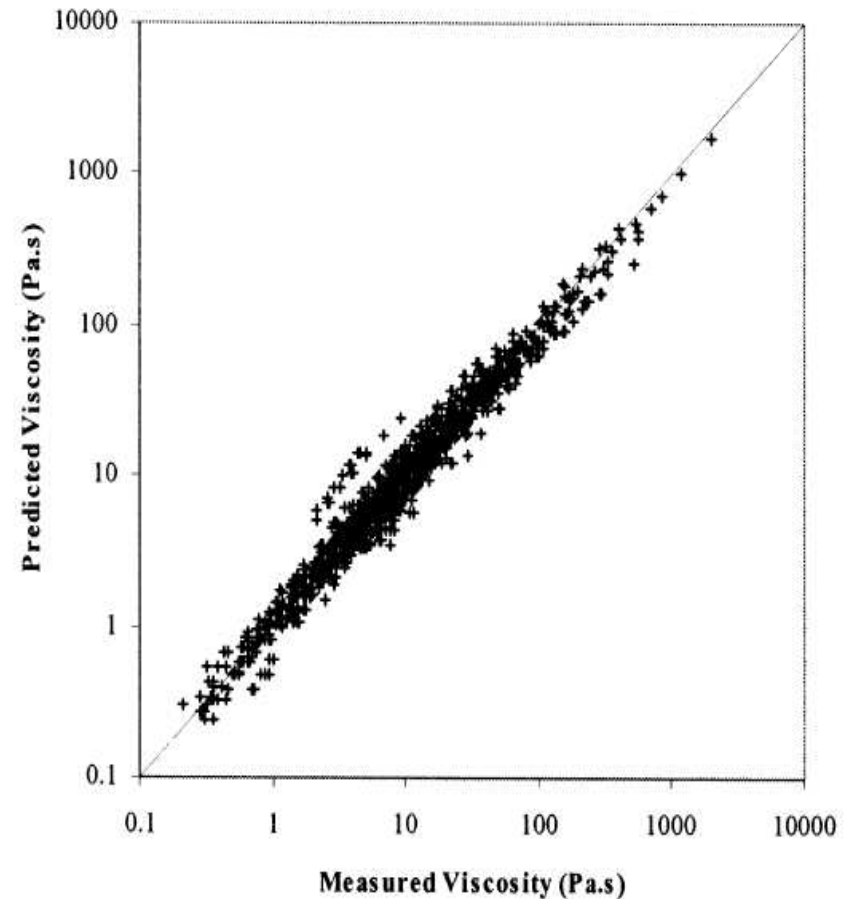
BROWNING method

$$\log\left(\frac{\eta}{T - T_s}\right) = \frac{14788}{T - T_s} - 10.931$$

$$T_s = 306.63 \ln(A) - 574.31$$

$$A = \frac{(3.19Si^{4+} + 0.855Al^{3+} + 1.6K^+) / (0.93Ca^{2+} + 1.50Fe^{n+} + 1.21Mg^{2+} + 0.69Na^+ + 1.35Mn^{n+} + 1.47Ti^{4+} + 1.91S^{2-})}{}$$

$$Si^{4+} + Al^{3+} + Ca^{2+} + Fe^{n+} + Mg^{2+} + Na^+ + K^+ + Mn^{n+} + Ti^{4+} + S^{2-} = 1$$





VISCOSITY OF SILICATE MELTS: SLAG RESULTS (Pa.s)

T (°C)	STOICH.	5.0 % C	7.5 % C	10.0 % C	TARGET
1300	0.567	0.678	0.710	0.712	<u>3.046</u>
1400	0.265	0.312	0.325	0.326	1.204
1500	0.133	0.154	0.160	0.161	0.523
1600	0.071	0.081	0.084	0.084	0.247
1700	0.040	0.045	0.047	0.047	0.125
1800	<u>0.024</u>	0.027	0.027	0.027	0.067



SURF. TENSION OF SILICATE MELTS (Dudek et al., 2009)

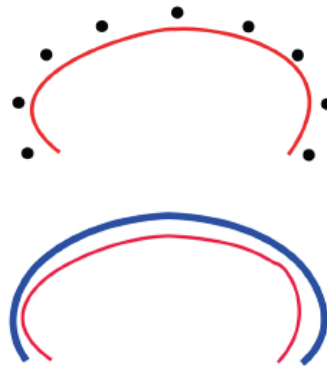
YOUNG-LAPLACE EQN.

$$p = \gamma \left(\frac{1}{R_1} + \frac{1}{R_2} \right) = 2\gamma H$$

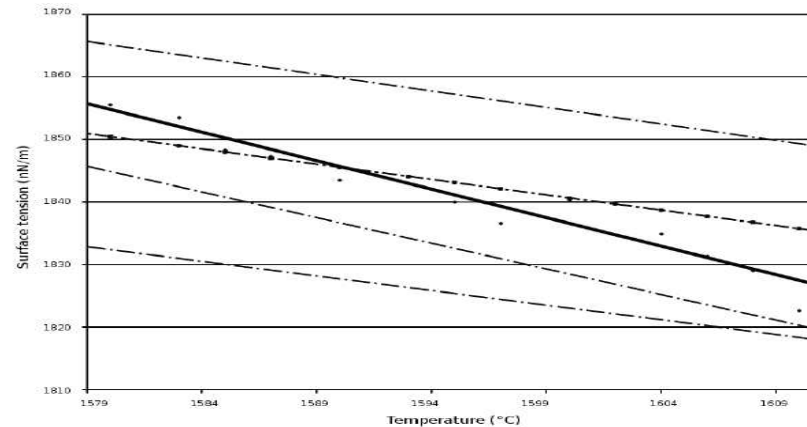


HIGH ACCURACY via ODE-BASED OPTIMIZATION

$$E(x_0, \theta, b, c) = \sum_{x \in \Omega} w(x) d^2(x, \mathcal{L}(x_0, \theta, b, c))$$



$$\begin{aligned} \frac{dx}{ds} &= \cos \varphi, \\ \frac{dy}{ds} &= \sin \varphi, \\ \frac{d\varphi}{ds} &= 2b + cy - \frac{\sin \varphi}{x} \end{aligned}$$





SURF. TENSION OF SILICATE MELTS: LITERATURE DATA

Surface Tension of CaO–Al₂O₃–SiO₂ Oxide Melts

I. A. Magidson, A. V. Basov, and N. A. Smirnov

Chemical compositions of the charges and surface tension σ of CaO–Al₂O₃–SiO₂ melts

Chemical composition, wt %			A, mN/m	B, mN/(m K)	σ_{1550} , mN/m	δ_{σ} , mN/m	Temperature range, °C
CaO	Al ₂ O ₃	SiO ₂					
60	30	10	674.5	0.094	503	0.6	1557–1415
55	35	10	679.3	0.0945	507	0.6	1583–1410
50	40	10	704.2	0.1065	510	0.45	1575–1420
45	45	10	712.8	0.109	514	0.8	1550–1410
60	25	15	719.7	0.1315	480	1.1	1590–1410
55	30	15	728.9	0.134	484.5	0.35	1585–1415
50	35	15	743.7	0.141	486.5	1.15	1540–1410
45	40	15	738.8	0.135	492.5	0.85	1595–1420
60	20	20	756.3	0.163	459	0.35	1575–1420
55	25	20	757.9	0.162	462.5	0.35	1585–1410
50	30	20	771.5	0.1675	466	0.7	1565–1420

Surface Tension of CaO–Al₂O₃, CaO–SiO₂, and CaO–Al₂O₃–SiO₂ Melts

N. A. Arutyunyan^a, A. I. Zaitsev^b, and N. G. Shaposhnikov^b

Table 1. Surface tension and molar volumes (m³/mol) $V = x[1 + (T - 1773) \times 10^{-4}] \times 10^{-6}$ of pure components [13]

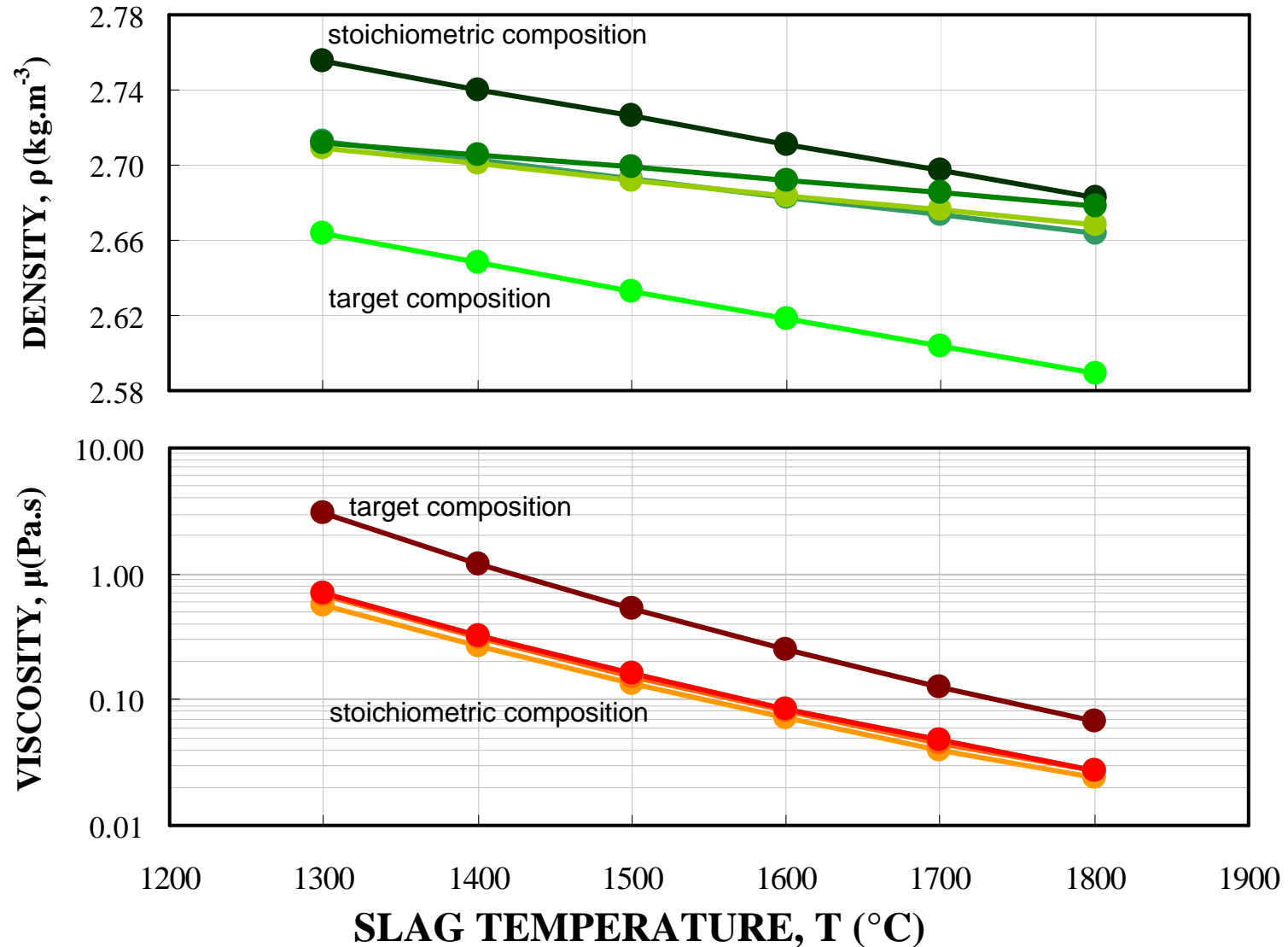
Component	σ , mN/m	x
CaO	$645.2 - 0.097(T - 2873)$	20.7
Al ₂ O ₃	$721.2 - 0.078(T - 2313)$	28.3
SiO ₂	$243.2 + 0.031T$	27.516

Table 2. Parameters characterizing excess Gibbs energy on the surface and molar surface of CaO–Al₂O₃–SiO₂ melt and its binary components

i CaO	j Al ₂ O ₃	k SiO ₂	L_{ijk}^{surf} , J/mol	¹ A	² A
				m ² /mol	
1	1	0	$95101 - 70T$		
1	0	1	$-56978 - 12.6T$	$-74851 - 9.1T$	-50632
2	0	2	-121900		
0	1	1	-37614	-1473.3	
1	1	1	63598		



SUMMARY OF TRANSPORT PROPERTY MODELING



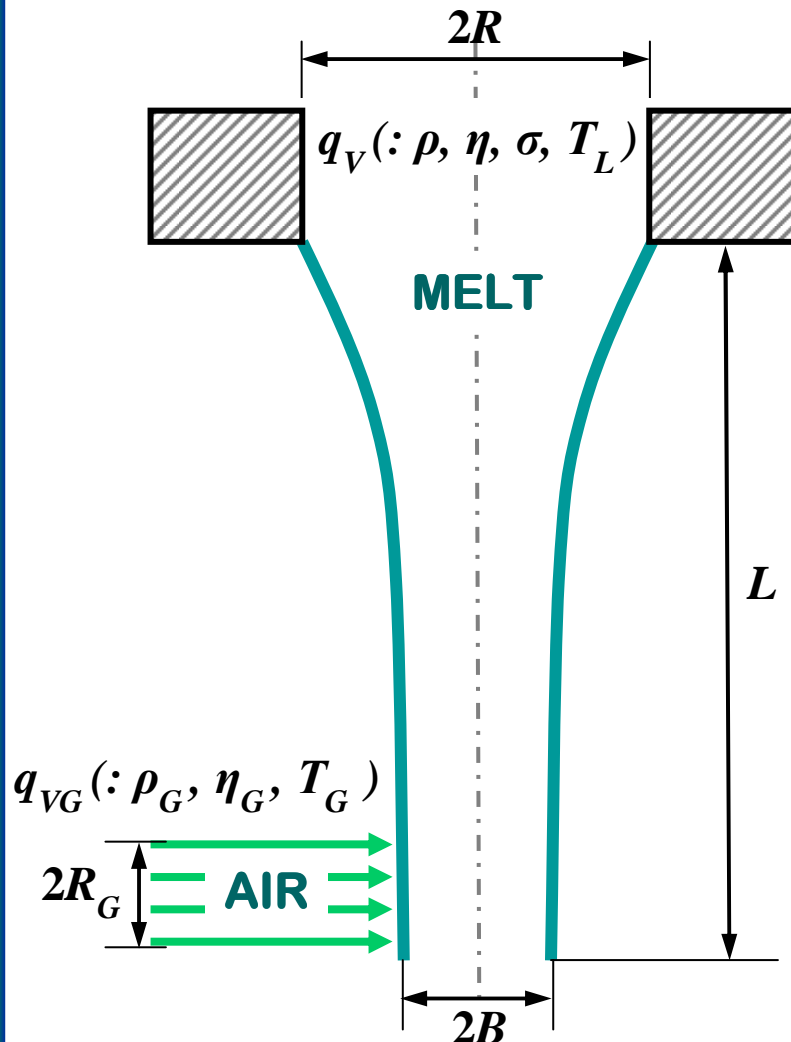


AGENDA

- Mineral wool fiberization - Mathematical modeling strategy
- Thermophysical properties of molten slag: Literature review
- Dimensional Analysis: Governing dimensionless numbers
- CFD analysis of nonisothermal vertical free surface flow
- Conclusions on process design and future research goals



MELT BLOW FIBERIZATION: OPERATING PRINCIPLE



GOVERNING PROCESS VARIABLES

melt density:	ρ (kg.m^{-3})
dynamic viscosity of the melt:	η ($\text{kg.m}^{-1}.\text{s}^{-1}$)
surface tension of the melt:	σ (kg.s^{-2})
radius of the orifice:	R (m)
final radius of the vertical stream:	B (m)
height of the vertical stream:	L (m)
radius of the impinging air jet:	R_G (m)
melt flow rate:	q_V ($\text{m}^3.\text{s}^{-1}$)
air density:	ρ_G (kg.m^{-3})
dynamic viscosity of air:	η_G ($\text{kg.m}^{-1}.\text{s}^{-1}$)
air flow rate:	q_{VG} ($\text{m}^3.\text{s}^{-1}$)
melt temperature:	T_L (K)
air temperature:	T_G (K)
temperature difference:	$\Delta T = T_L - T_G$ (K)



MELT BLOW FIBERIZATION: DIMENSIONAL ANALYSIS

- Dimensional system (M, L, T, Θ):

	ρ	R	η	T_L	L	σ	q_V	B	ΔT	q_{VG}	R_G	η_G	ρ_G	T_G	d_F
M	1	0	1	0	0	1	0	0	0	0	0	1	1	0	0
L	-3	1	-1	0	1	0	3	1	0	3	1	-1	-3	0	1
T	0	0	-1	0	0	-2	-1	0	0	-1	0	-1	0	0	0
Θ	0	0	0	1	0	0	0	0	1	0	0	0	0	1	0

$$Z_1 = M + T$$

$$Z_2 = 3M + L + 2T$$

$$Z_3 = -T$$

$$Z_4 = \Theta$$

	ρ	R	η	T_L	L	σ	q_V	B	ΔT	q_{VG}	R_G	η_G	ρ_G	T_G	d_F
Z_1	1	0	0	0	0	-1	-1	0	0	-1	0	0	1	0	0
Z_2	0	1	0	0	1	-1	1	1	0	1	1	0	0	0	1
Z_3	0	0	1	0	0	2	1	0	0	1	0	1	0	0	0
Z_4	0	0	0	1	0	0	0	0	1	0	0	0	0	1	0

CORE MATRIX

RESIDUAL MATRIX



MELT BLOW FIBERIZATION: DIMENSIONLESS NUMBERS

$$N_1 = \frac{L}{R}, \quad N_2 = \frac{\rho R \sigma}{\eta^2}, \quad N_3 = \frac{\rho q_V}{\eta R}, \quad N_4 = \frac{B}{R}, \quad N_5 = \frac{\Delta T}{T_L},$$

$$N_6 = \frac{\rho q_{VG}}{\eta R}, \quad N_7 = \frac{R_G}{R}, \quad N_8 = \frac{\eta_G}{\eta}, \quad N_9 = \frac{\rho_G}{\rho}, \quad N_{10} = \frac{T_G}{T_L}, \quad N_{11} = \frac{d_F}{R}$$

Derivation of equivalent dimensionless numbers

$$M_1 = \frac{N_1^2}{N_2} = \frac{\eta^2}{\rho R \sigma}, \quad M_2 = \frac{N_3}{\sqrt{N_2}} \frac{1}{N_4} = \frac{q_V}{B} \sqrt{\frac{\rho}{\sigma R}}, \quad M_3 = \frac{N_6}{\sqrt{N_2}} \frac{1}{N_4} = \frac{q_{VG}}{B} \sqrt{\frac{\rho}{\sigma R}}, \quad M_4 = N_4 = \frac{B}{R},$$

$$M_5 = N_5 = \frac{\Delta T}{T_L}, \quad M_6 = \frac{N_3}{N_6} = \frac{q_V}{q_{VG}}, \quad M_7 = N_7 = \frac{R_G}{R}, \quad M_8 = N_8 = \frac{\eta_G}{\eta}$$

$$M_9 = N_9 = \frac{\rho_G}{\rho}, \quad M_{10} = N_{10} = \frac{T_G}{T_L}, \quad M_{11} = N_{11} = \frac{d_V}{R}$$



CHARACTERISTIC DIMENSIONLESS NUMBERS

- characteristic dimensionless flow number:

$$\Pi_3 = q_V^* = M_2 = \frac{q_V}{B} \sqrt{\frac{\rho}{\sigma R}} ;$$

- characteristic dimensionless viscosity number:

$$\Pi_4 = Z = M_1 = \frac{\eta^2}{\rho R \sigma} ; \quad \text{(inverse Laplace number)}$$

- characteristic dimensionless temperature number:

$$\Pi_5 = T^* = M_5 = \frac{\Delta T}{T_L} ;$$

- characteristic dimensionless flow number: **(Lubanska number, 1970)**

$$\Pi_6 = Lu = \left(1 + \frac{q_V \rho}{q_{VG} \rho_G} \right) \frac{v}{v_G} = \left[\left(1 + \frac{q_m}{q_{mG}} \right) \frac{v}{v_G} \right] = [(1 + M_6 \cdot M_7) M_8 \cdot M_9] .$$



FIBRE SIZE: THE DATA-DRIVEN STATISTICAL MODEL

gradual
simplification

$$M_{11} = \frac{d_V}{R} = \frac{d_V}{R} (M_1, M_2, M_3, M_4, M_5, M_6, M_7, M_8, M_9, M_{10}, M_{11})$$

$$M_{11} = \frac{d_V}{R} = \frac{d_V}{R} (M_1, M_2, M_3, M_4, M_5, M_6, M_7, M_8, M_9)$$

$$d_F = a_0 \cdot \Pi_1^{a_1} \cdot \Pi_2^{a_2} \cdot \Pi_3^{a_3} \cdot \Pi_4^{a_4} \cdot \Pi_5^{a_5} \cdot \Pi_6^{a_6}$$

a_i ($i = 0$ to 6) are the parametric constants of the multiple regression model (determined by statistical methods on the basis of an experimental dataset)



IA-based THERMOPHYSICAL PROPERTY BOUNDS: DATA

	<i>MIN</i>	<i>MAX</i>	<i>UNIT</i>
SLAG DENSITY (ρ)	$2.589 \cdot 10^{+3}$	$2.755 \cdot 10^{+3}$	(kg.m ⁻³)
SLAG VISCOSITY (μ)	$2.400 \cdot 10^{-2}$	$3.046 \cdot 10^0$	(Pa.s)
SLAG SURF. TENSION (σ)	$3.680 \cdot 10^{-1}$	$5.100 \cdot 10^{-1}$	(N.m ⁻¹)
SLAG JET VELOCITY (V)	$5.000 \cdot 10^{-2}$	$2.000 \cdot 10^{-1}$	(m.s ⁻¹)
SLAG DROP VELOCITY (v)	$5.000 \cdot 10^{-1}$	$2.000 \cdot 10^0$	(m.s ⁻¹)
SLAG JET DIAMETER (D)	$5.000 \cdot 10^{-2}$	$2.000 \cdot 10^{-1}$	(m)
SLAG DROP DIAMETER (d)	$1.000 \cdot 10^{-3}$	$1.000 \cdot 10^{-2}$	(m)



IA-based DIMENSIONLESS NUMBER BOUNDS: RESULTS

(with respect to molten slag jet)

MIN

MAX

REYNOLDS (Re)	$Re = \frac{\rho V L}{\mu}$	$2.125 \cdot 10^0$	$4.592 \cdot 10^{+3}$
CAPILLARY (Ca)	$Ca = \frac{\mu V}{\sigma}$	$2.353 \cdot 10^{-3}$	$1.655 \cdot 10^0$
OHNESORGE (Oh)	$Oh = \frac{\mu}{\sqrt{\rho \sigma L}}$	$1.432 \cdot 10^{-3}$	$4.413 \cdot 10^{-1}$
LAPLACE (La)	$La = \frac{\sigma \rho L}{\mu^2}$	$5.134 \cdot 10^0$	$4.879 \cdot 10^{+5}$
WEBER (We)	$We = \frac{\rho v^2 l}{\sigma}$	$6.346 \cdot 10^{-1}$	$5.989 \cdot 10^{+1}$



IA-based DIMENSIONLESS NUMBER BOUNDS: RESULTS

(with respect to molten slag drop)

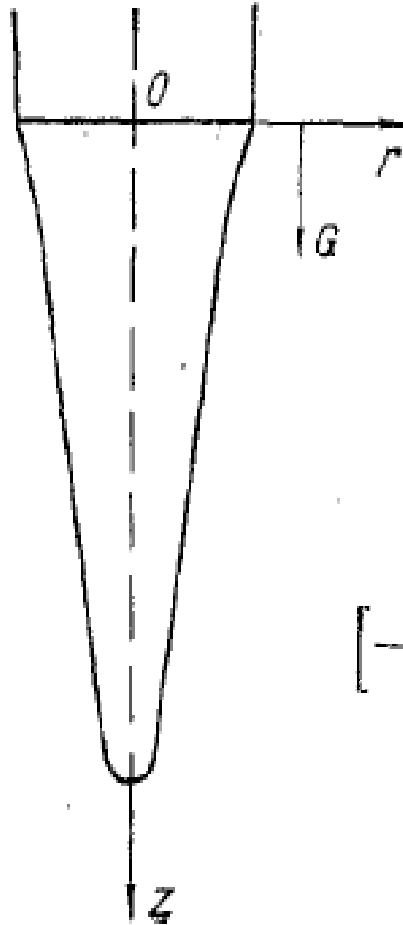
MIN

MAX

REYNOLDS (Re)	$Re = \frac{\rho V L}{\mu}$	$4.250 \cdot 10^{-1}$	$2.296 \cdot 10^{+3}$
CAPILLARY (Ca)	$Ca = \frac{\mu V}{\sigma}$	$2.353 \cdot 10^{-2}$	$1.655 \cdot 10^{+1}$
OHNESORGE (Oh)	$Oh = \frac{\mu}{\sqrt{\rho \sigma L}}$	$6.403 \cdot 10^{-3}$	$3.121 \cdot 10^0$
LAPLACE (La)	$La = \frac{\sigma \rho L}{\mu^2}$	$1.027 \cdot 10^{-1}$	$2.439 \cdot 10^{+4}$
WEBER (We)	$We = \frac{\rho v^2 l}{\sigma}$	$1.269 \cdot 10^0$	$2.995 \cdot 10^{+2}$



THE COOLED VERTICAL JET MODEL (Epikhin et al., 1982)



$$\frac{du_j}{dt} = -\nabla p_j + \frac{v_j}{v_1 \text{Re}} \Delta u_j + \frac{2-j}{\text{Fr}} k_x \quad (1)$$

$$\nabla \cdot u_j = 0, \quad \frac{d\theta_j}{dt} = \frac{\kappa_j}{\alpha_1 \text{Pe}} \Delta \theta_j \quad (j=1, 2), \quad (2)$$

$$\frac{dh}{dt} = v, \quad y = h(x). \quad (3)$$

$$v_1 = u_{1y} = \theta_{1y} = 0, \quad y = 0, \quad (4)$$

$$[u]_2^1 = 0, \quad [v]_2^1 = 0, \quad (5)$$

$$\left[\frac{\mu}{\mu_1} \left\{ u_y + v_x + 2b \left(2v_y + \frac{v}{y} \right) \frac{1}{1-b^2} \right\} \right]_2^1 = 0, \quad (6)$$

$$\left[-\frac{\rho}{\rho_1} p + 2 \frac{v}{v_1} \left\{ (1+b^2)v_y + b^2 \frac{v}{y} \right\} \frac{1}{(1-b^2)\text{Re}} \right]_2^1 = -\frac{2}{\text{We} R_s}, \quad (7)$$

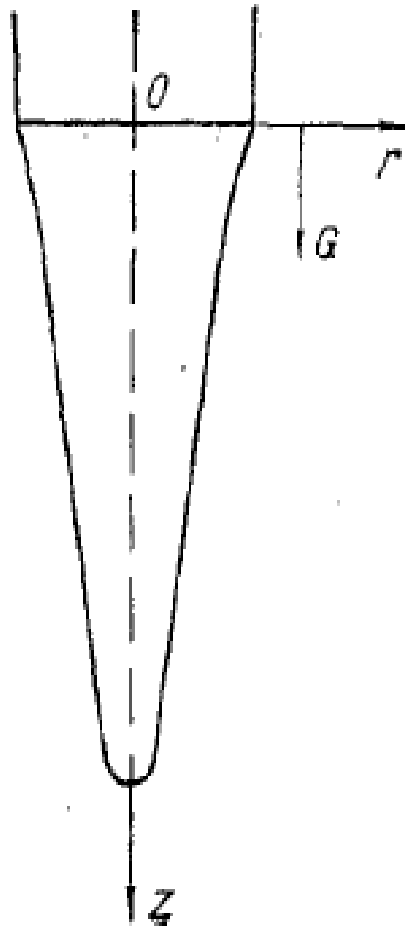
$$[\theta]_2^1 = 0, \quad (8)$$

$$\left[\frac{\lambda}{\lambda_1} \frac{\theta_y - b\theta_x}{\sqrt{1+b^2}} + \varepsilon \text{Bo} \left(\theta + \frac{T_E^0}{\Delta T} \right)^4 \right]_2^1 = 0, \quad (9)$$

$$u_2 \rightarrow U_E(x), \quad \theta_2 \rightarrow \theta_E(x), \quad y \rightarrow \infty \quad (|b| < 1). \quad (10)$$



THE REDUCED MODEL w/ DIMENSIONLESS NUMBERS



$$\frac{1}{Fr} = \frac{(1-\rho_0)GR}{U^2}, \quad Re = \frac{\rho_1 RU}{\mu_1}, \quad (11)$$

$$Pe = \frac{\rho_1 C_{V1} RU}{\lambda_1}, \quad Bo = \frac{\sigma R (\Delta T)^3}{\lambda_1}, \quad We = \frac{\gamma}{\rho_1 U^2 R},$$

$$(x, y) = (z, r) R^{-1}, \quad (u, U_E, v) = (u_*, U_{*E}, v_*) U^{-1},$$

$$\kappa_j = \frac{\lambda_j}{\rho_j C_{Vj}}, \quad \rho_j = \frac{\rho_{*j}}{\rho_j U^2}, \quad \rho_0 = \frac{\rho_2}{\rho_1} \quad (j = 1, 2),$$

$$\theta = \frac{T - T_E^0}{\Delta T}, \quad \Delta T = T^0 - T_E(0), \quad T_E^0 = T_E(0), \quad (12)$$

$$\frac{2}{R_S} = \left\{ \frac{1}{h} - \frac{b}{1+b^2} \right\} \frac{1}{\sqrt{1+b^2}}, \quad b = \dot{h}(x) = \frac{dh}{dx}.$$



FREE SURFACE SHAPE OF JETS (Georgiou et al., 1988)

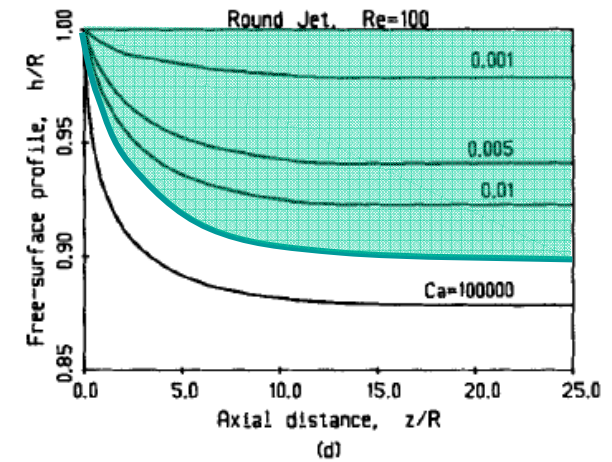
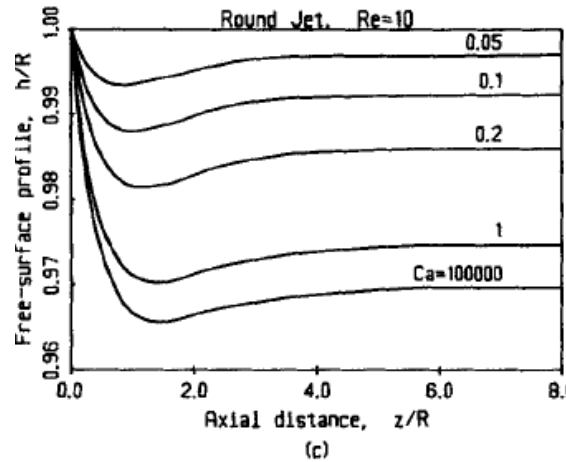
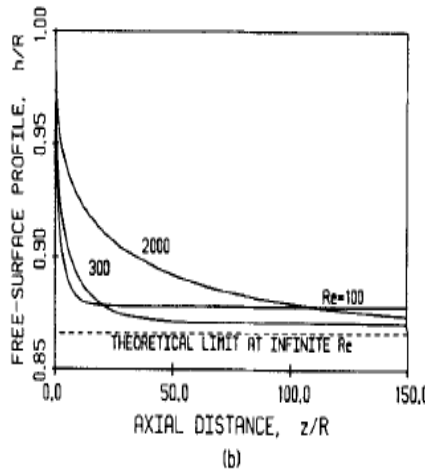
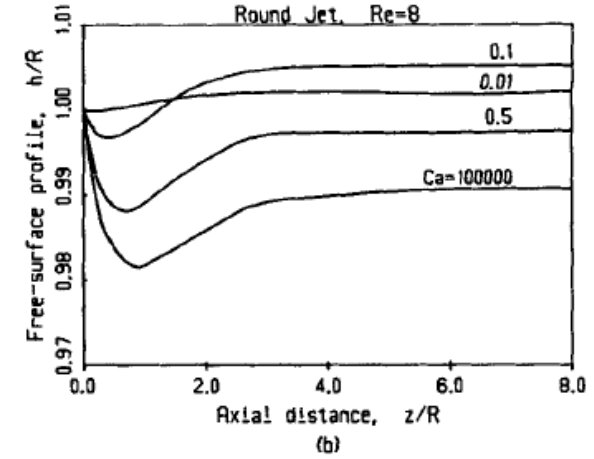
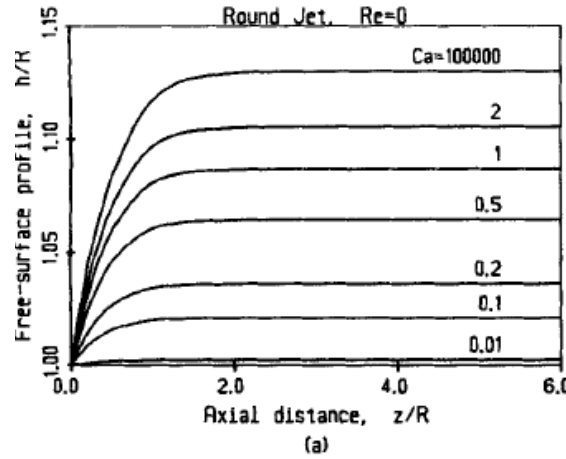
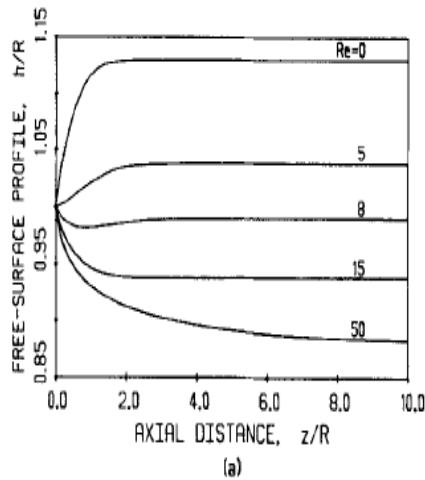


Figure 1. Predicted free-surface profiles of a round jet.
Various $Re = \rho UR/\mu$, zero surface tension

Figure 2. Predicted free-surface profiles of a round jet.
Various $Re = \rho UR/\mu$, $Ca = \mu U/\sigma$

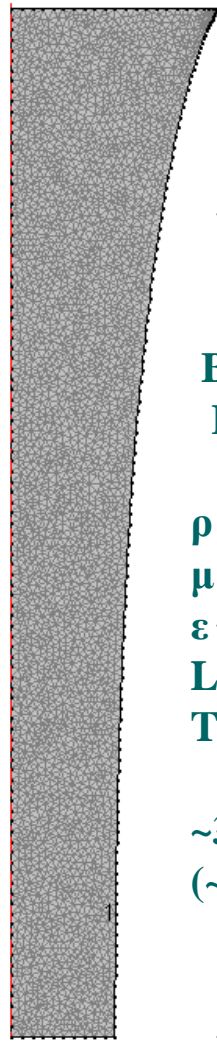


AGENDA

- Mineral wool fiberization - Mathematical modeling strategy
- Thermophysical properties of molten slag: Literature review
- Dimensional Analysis: Governing dimensionless numbers
- **CFD analysis of nonisothermal vertical free surface flow**
- Conclusions on process design and future research goals



CFD ANALYSIS: COMPUTATIONAL DOMAIN & BASE CASE

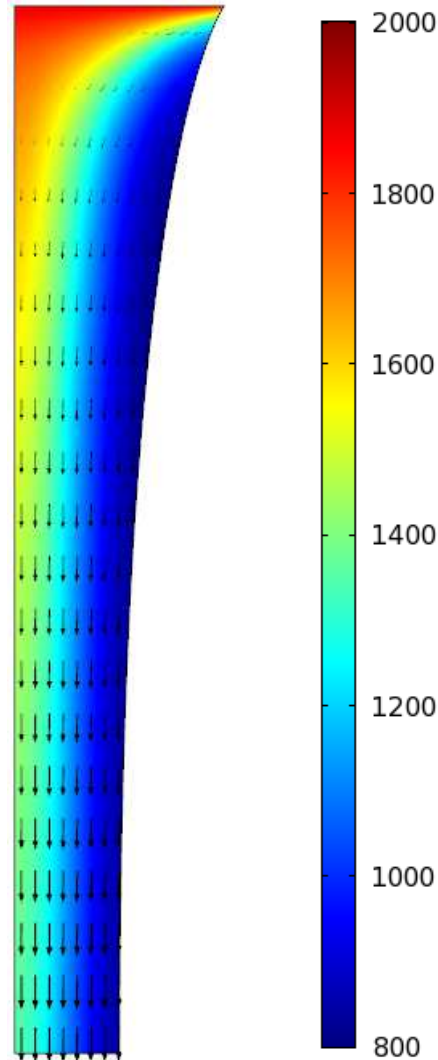


BASE CASE CFD PARAMETERS

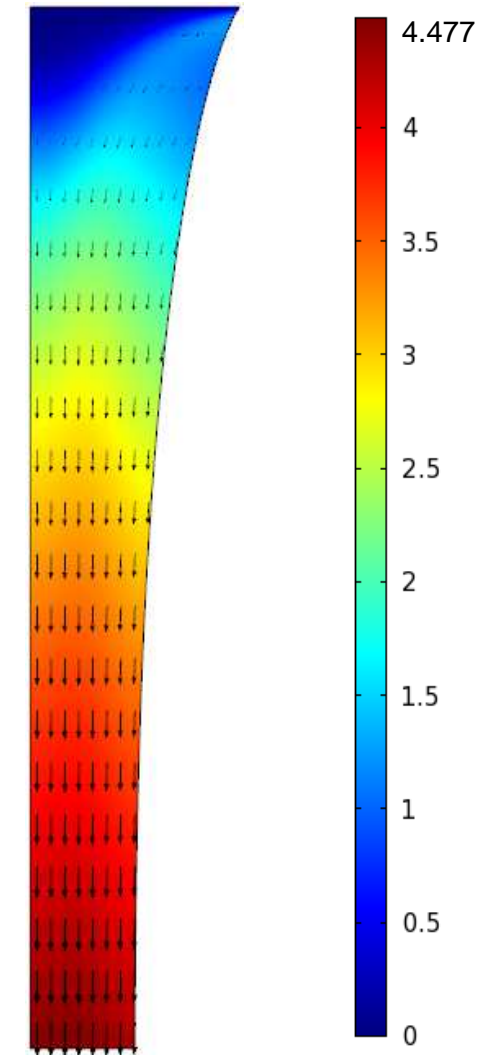
$\rho = 2500 \text{ kg.m}^{-3}$
 $\mu = 1.0 \text{ Pa.s}$
 $\varepsilon = 0.90$
 $L = 1.0 \text{ m}$
 $T_{in} = 1873.15 \text{ K}$

~3000 tet. elements
(~12000 FEM DOF)

COMPUTATIONAL GRID



TEMPERATURE (T)

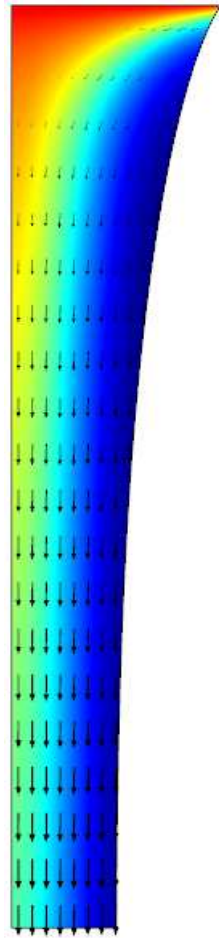


VELOCITY (U)



CFD ANALYSIS: EFFECT OF SLAG DENSITY (ρ)

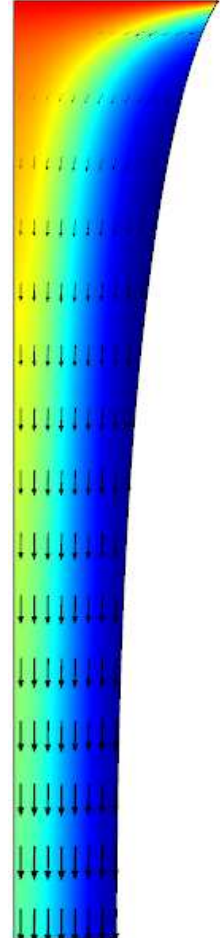
$\rho = 2500 \text{ kg.m}^{-3}$



$T_{\text{out,min}} = 800 \text{ K}$

$T_{\text{out,max}} = 1355 \text{ K}$

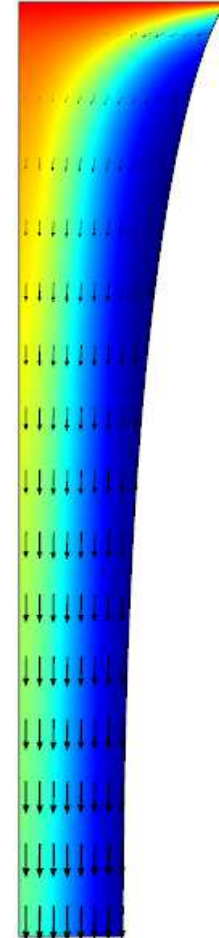
$\rho = 2600 \text{ kg.m}^{-3}$



799 K

1360 K

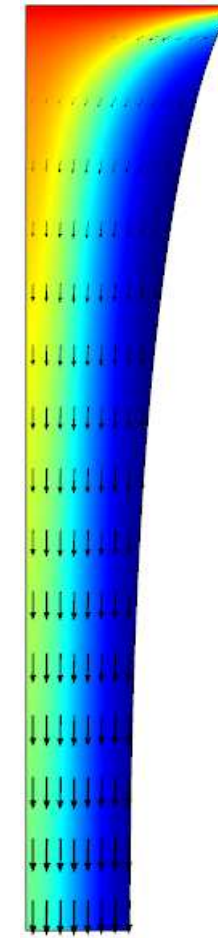
$\rho = 2700 \text{ kg.m}^{-3}$



798 K

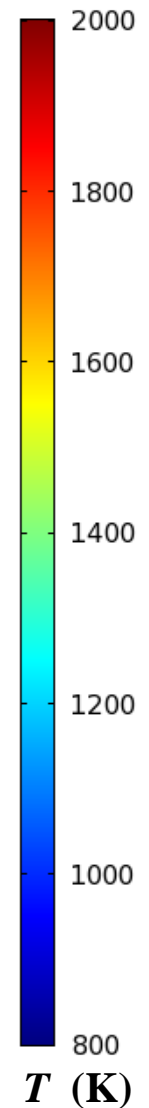
1367 K

$\rho = 2800 \text{ kg.m}^{-3}$



796 K

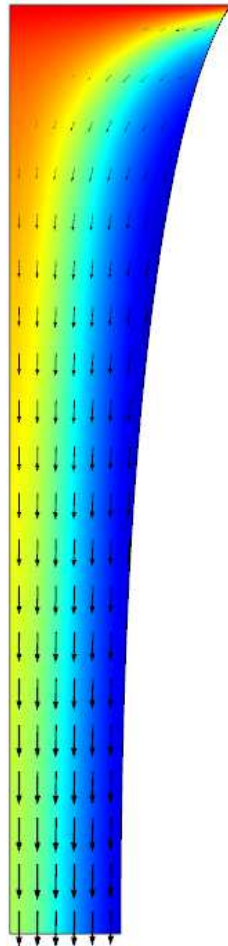
1374 K





CFD ANALYSIS: EFFECT OF SLAG VISCOSITY (μ)

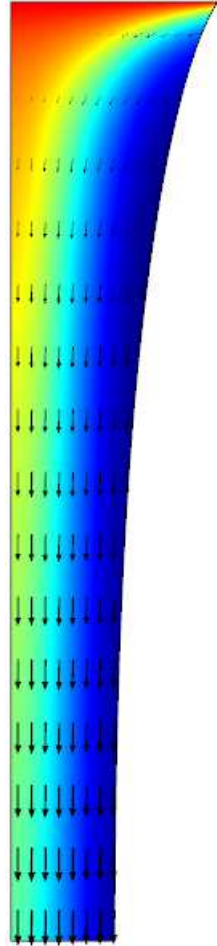
$\mu = 0.5 \text{ Pa}\cdot\text{s}$



$T_{\text{out,min}} = 848 \text{ K}$

$T_{\text{out,max}} = 1380 \text{ K}$

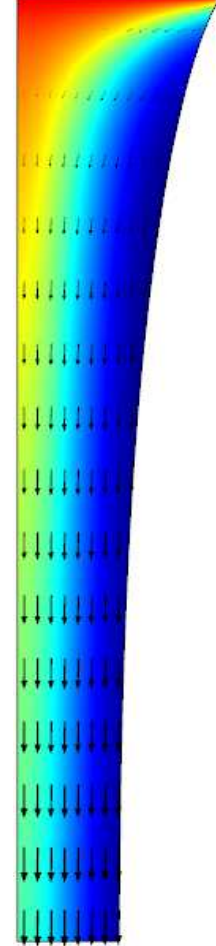
$\mu = 1.0 \text{ Pa}\cdot\text{s}$



800 K

1355 K

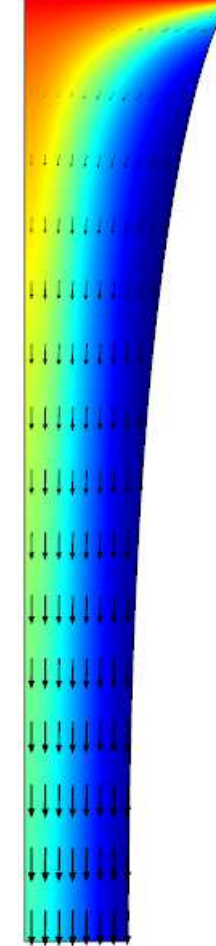
$\mu = 2.0 \text{ Pa}\cdot\text{s}$



802 K

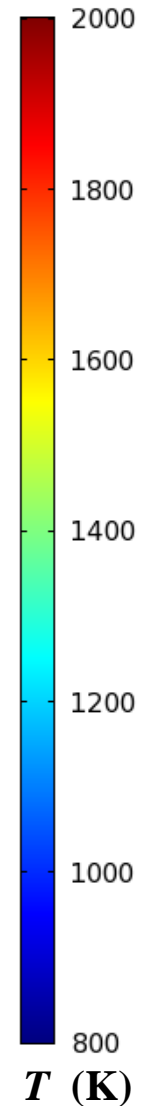
1340 K

$\mu = 3.0 \text{ Pa}\cdot\text{s}$



803 K

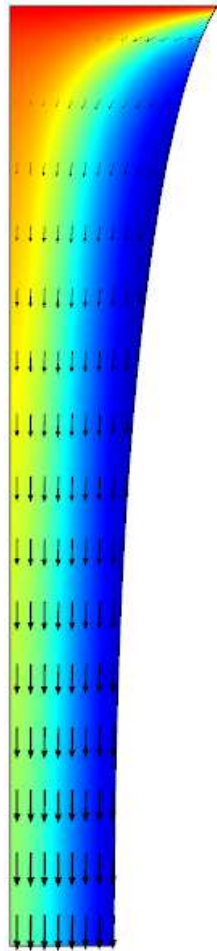
1325 K





CFD ANALYSIS: EFFECT OF SLAG EMISSIVITY (ϵ)

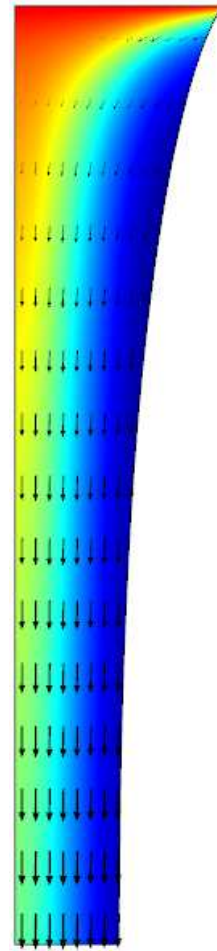
$\epsilon = 0.70$



$T_{\text{out,min}} = 860 \text{ K}$

$T_{\text{out,max}} = 1401 \text{ K}$

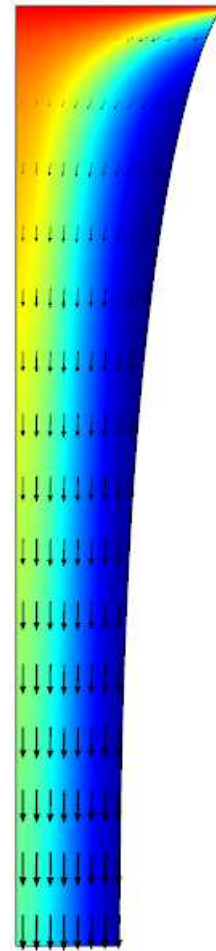
$\epsilon = 0.80$



828 K

1377 K

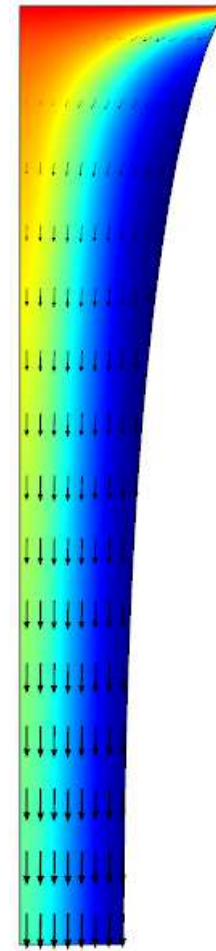
$\epsilon = 0.90$



800 K

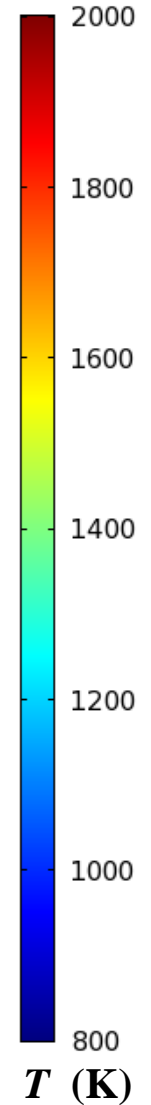
1355 K

$\epsilon = 0.95$



788 K

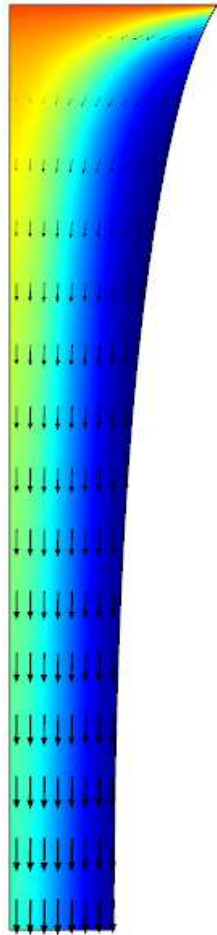
1346 K





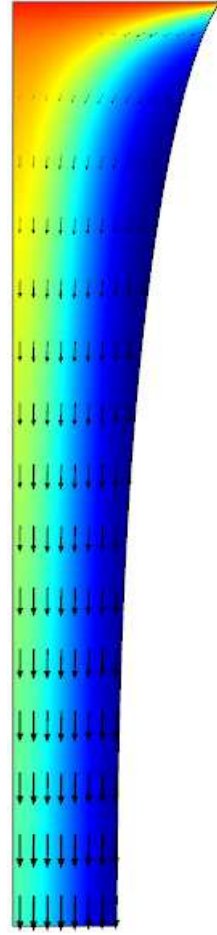
CFD ANALYSIS: EFFECT OF LADLE TEMPERATURE

$T_{in} = 1773.15 \text{ K}$



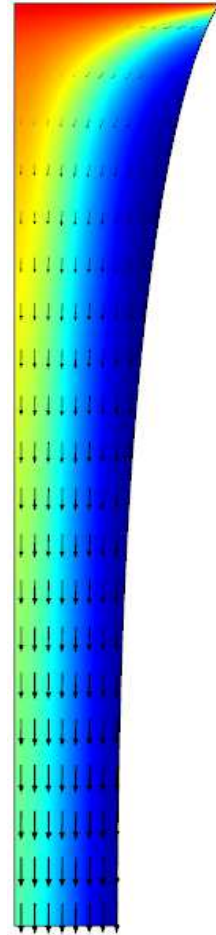
$T_{out,min} = 795 \text{ K}$
 $T_{out,max} = 1312 \text{ K}$

$T_{in} = 1823.15 \text{ K}$



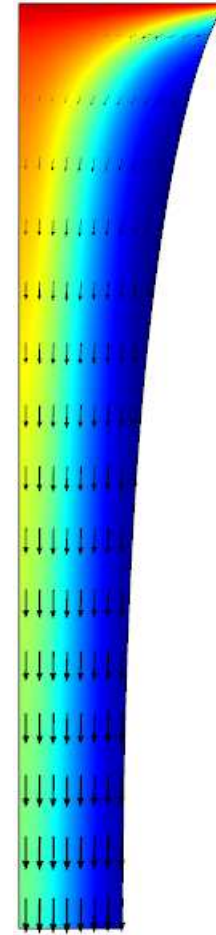
798 K
1334 K

$T_{in} = 1873.15 \text{ K}$

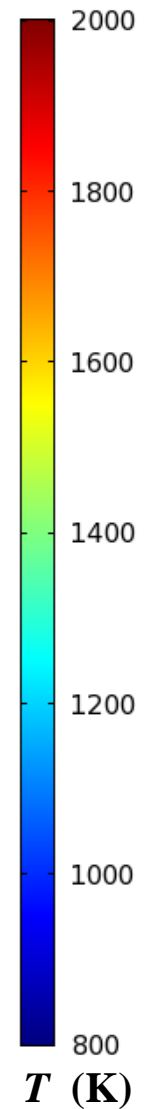


800 K
1355 K

$T_{in} = 1923.15 \text{ K}$



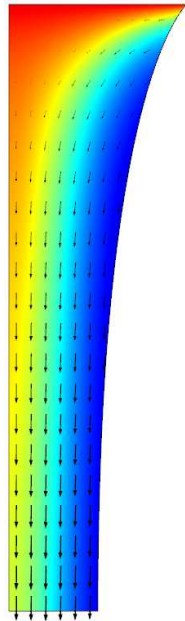
803 K
1378 K



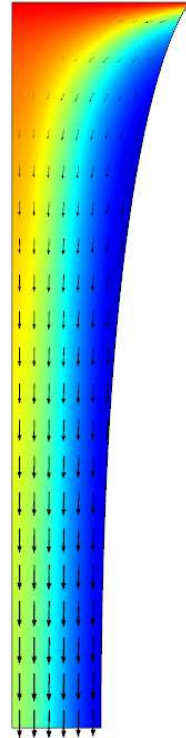


CFD ANALYSIS: EFFECT OF DISTANCE (L , JET HEIGHT)

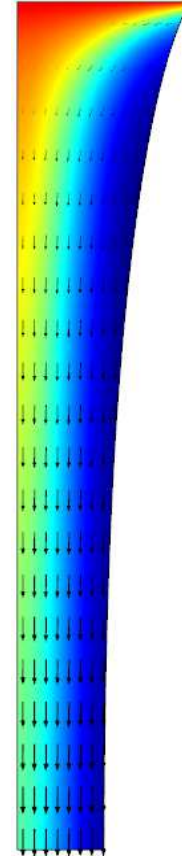
$L = 0.60$ m



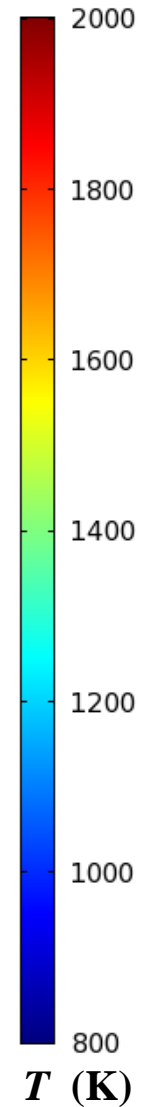
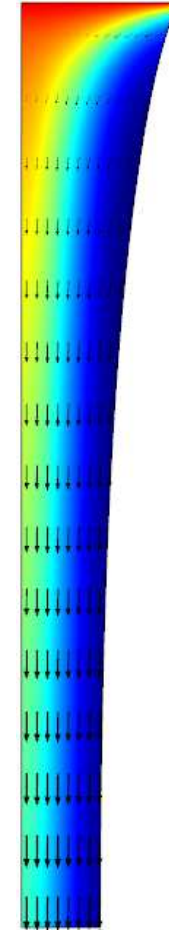
$L = 0.80$ m



$L = 1.00$ m



$L = 1.20$ m



$T_{out,min} = 921$ K

889 K

800 K

780 K

$T_{out,max} = 1490$ K

1447 K

1355 K

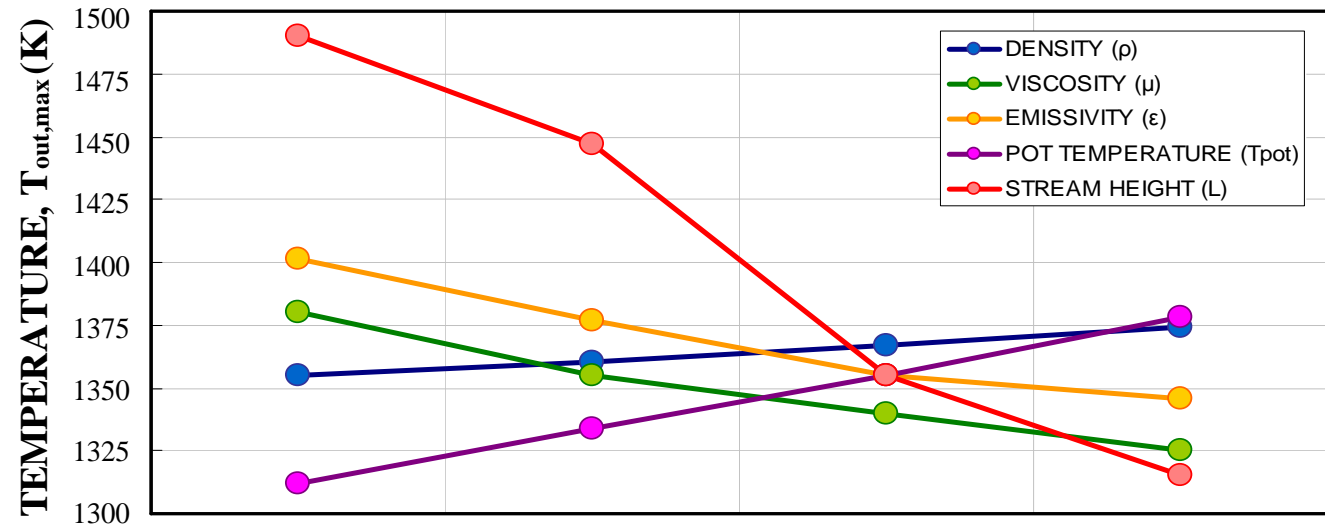
1315 K

T (K)

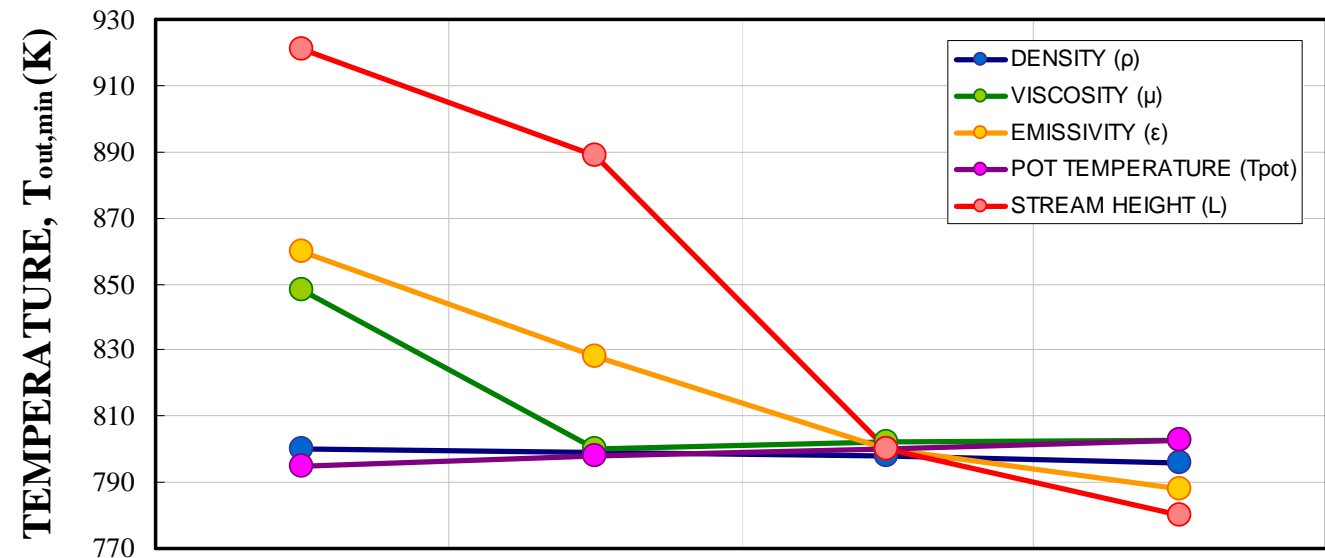


CFD ANALYSIS: PARAMETRIC SENSITIVITY SUMMARY

**VERTICAL
SLAG STREAM
BOTTOM
TEMPERATURE
(core = maximum)**



**VERTICAL
SLAG STREAM
BOTTOM
TEMPERATURE
(skin = minimum)**





MOLTEN SLAG DISINTEGRATION BY GAS (Silaev, 1966)

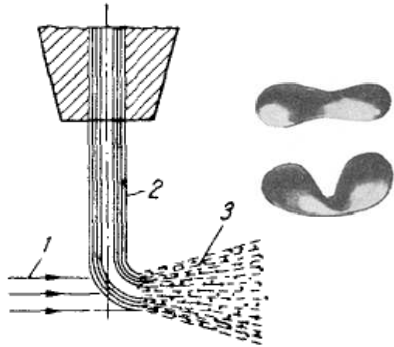


Fig. 1. Scheme of engagement between liquid metal stream and transverse gas jet: 1) gas jet; 2) liquid metal stream; 3) atomization zone.

$$\frac{\bar{a}}{D_0} = F(We, Lp, M, N) \quad (\text{molten stream})$$

$$\frac{D'_0}{R_0} = \sqrt[3]{V + \Pi} We^{-\frac{1}{3}}$$

$$\frac{\bar{a}}{D_0} = F(We, Lp) \quad (\text{isolated drop})$$

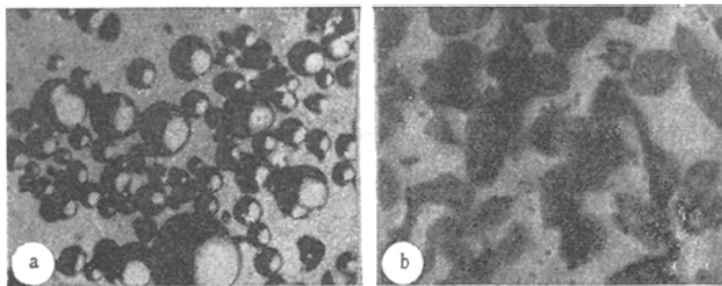


Fig. 5. Geometry of particles of Fe-Cr base alloy powder, $\times 126$: a) spherical particle shape; b) irregular (angular) particle shape.

$$We = \frac{U_g^2 \rho_g D_0}{\sigma_g} \quad - \text{is the Weber number}$$

$$Lp = \frac{\mu_1^{g\sim}}{\sigma_1 \rho_1 D_0} \quad - \text{is the Laplace number}$$



MINERAL FIBRE LENGTH VARIATION (Kulago, 1986)

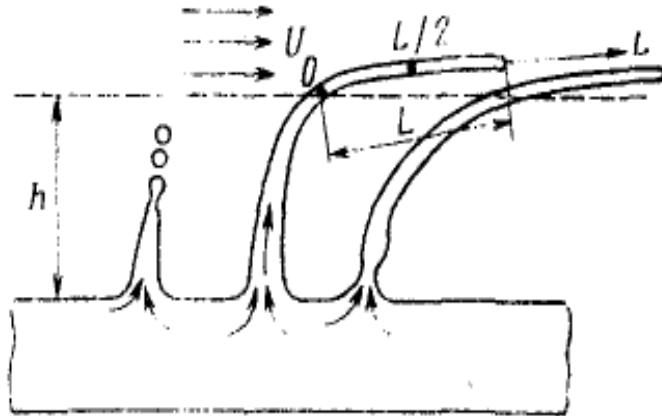


Fig. 1. Diagram of the perturbation of the surface of a melt: h) depth of boundary layer of gas; U) velocity of oncoming gas flow; L) length of solidifying section of fiber; 0) origin of coordinates; the straight arrows denote the direction of the gas flow; the curves arrows, the direction of movement of the melt from the layer.

Length of obtained fibres:

$$L = \frac{3}{2} \frac{1}{C_f} \frac{\rho_f}{\rho_g} d.$$

Exptl. data: $L_{\text{fibers}} = 5-6 \text{ cm } (\pm 20\%)$

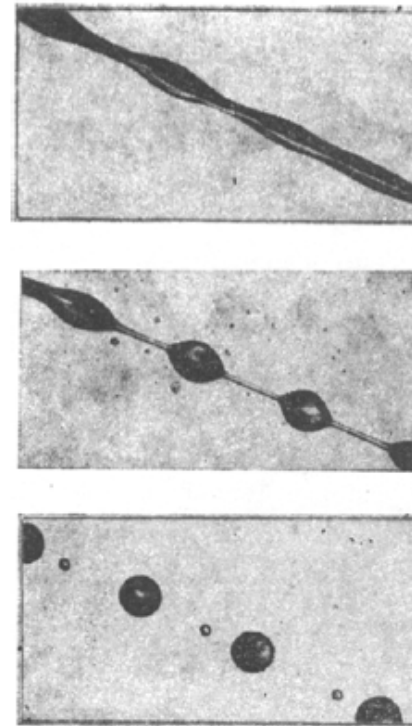


Fig. 2

Fig. 2. Decay of unperturbed surface of a jet of MV-3 oil in air for various sections: Reynold's No., $Re = 29.87$; Weber's No., $We = 1244$; $\rho_f = 680 \text{ kg/m}^3$; dynamic coefficient of viscosity of the oil $\mu_f = 1.69 \cdot 10^{-2} \text{ kg/(m}\cdot\text{sec)}$; $\sigma = 21.4 \cdot 10^{-3} \text{ N/m}$.

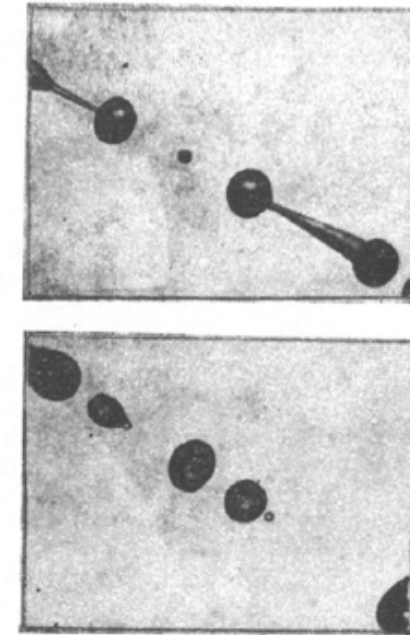


Fig. 3

Fig. 3. Decay of slightly perturbed jet of VM-3 oil in various sections; the applied perturbations were random; the numerical data is the same as in Fig. 2.



AGENDA

- Mineral wool fiberization - Mathematical modeling strategy
- Thermophysical properties of molten slag: Literature review
- Dimensional Analysis: Governing dimensionless numbers
- CFD analysis of nonisothermal vertical free surface flow
- Conclusions on process design and future research goals



CONCLUSIONS

- Mathematical modeling strategy for mineral wool fiberization
 - Multiphase mass and heat flow study in three (3) distinct zones
- Systematic for multiphase mass and heat flow CFD modeling
 - Thermophys. property, multiphase flow, fiber processing literature
- Thermophysical properties (ρ , μ , σ) are crucial (already investigated)
 - Temperature- & composition- dep. models yield ρ - μ - σ variation ranges
- Dimensional Analysis employed to identify key dim/less numbers
 - Reynolds, Weber, Capillary and Laplace numbers govern fiberization
 - Interval Arithmetic (IA) provides fast computation of respective bounds
- Sensitivity CFD analysis of exit temperature profile w.r.t. parameters
 - Emissivity, viscosity, jet size are pivotal; other phys. properties weaker



ACKNOWLEDGEMENTS

